

# Engineering Gac/Rsm Signaling Cascade for Optogenetic Induction of the Pathogenicity Switch in *Pseudomonas aeruginosa*

Xinyi Cheng,<sup>#</sup> Lu Pu,<sup>#</sup> Shengwei Fu,<sup>#</sup> Aiguo Xia, Shuqiang Huang, Lei Ni, Xiaochen Xing, Shuai Yang,\* and Fan Jin\*



Cite This: <https://doi.org/10.1021/acssynbio.1c00075>



Read Online

ACCESS |



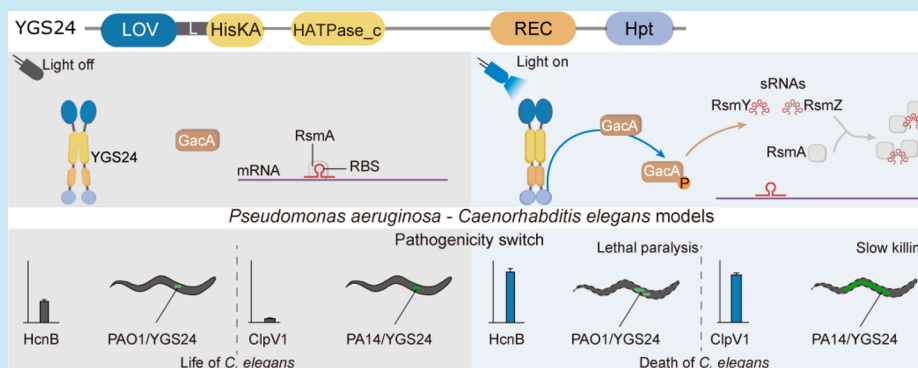
Metrics & More



Article Recommendations



Supporting Information



**ABSTRACT:** Bacterial pathogens operate by tightly controlling the pathogenicity to facilitate invasion and survival in host. While small molecule inducers can be designed to modulate pathogenicity to perform studies of pathogen–host interaction, these approaches, due to the diffusion property of chemicals, may have unintended, or pleiotropic effects that can impose limitations on their use. By contrast, light provides superior spatial and temporal resolution. Here, using optogenetics we reengineered GacS of the opportunistic pathogen *Pseudomonas aeruginosa*, signal transduction protein of the global regulatory Gac/Rsm cascade which is of central importance for the regulation of infection factors. The resultant protein (termed YGS24) displayed significant light-dependent activity of GacS kinases in *Pseudomonas aeruginosa*. When introduced in the *Caenorhabditis elegans* host systems, YGS24 stimulated the pathogenicity of the *Pseudomonas aeruginosa* strain PAO1 in a brain–heart infusion and of another strain, PA14, in slow killing media progressively upon blue-light exposure. This optogenetic system provides an accessible way to spatiotemporally control bacterial pathogenicity in defined hosts, even specific tissues, to develop new pathogenesis systems, which may in turn expedite development of innovative therapeutics.

**KEYWORDS:** Optogenetics, *Pseudomonas aeruginosa*, Gac/Rsm cascade, *Caenorhabditis elegans*, Pathogenicity control

The conditions of the host, the pathogen, and the environment determine the result of a host–pathogen interaction.<sup>1,2</sup> Host–pathogen interactions are important to our understanding of the mechanisms of infectious disease, including its treatment and prevention. Besides, the location and timing of invasion or colonization and their subsequent mode of action in host decide the pathogen’s success of infection. However, there are few methods that provide precise spatiotemporal control of infection. For instance, the injection systems applied to most host–pathogen interactions are not adequate for imaging the very early time course of infection due to the inevitable time delays of preparation of bringing a pathogen in contact with host cells. Other inoculation methods such as feeding assay and immersion infection are also limited in controlling the occurrence of infection in a defined location or tissue at specific times in intact systems.<sup>3–5</sup> Accordingly,

these techniques do not allow tracking the dynamics of host–pathogen interactions with spatiotemporal precision.

A promising approach to address the limitations is to couple the pathogenicity of bacteria to light signals. Light has advantages over chemical means of control of biological processes as it is noninvasive, has low toxicity, and most crucial, provides superior spatial and temporal resolution.<sup>6</sup> To capitalize on these favorable properties, we aim to develop a light-controlled system by incorporating photoactive allosteric modulators semisynthetically to enable previously unrivaled

**Received:** February 26, 2021

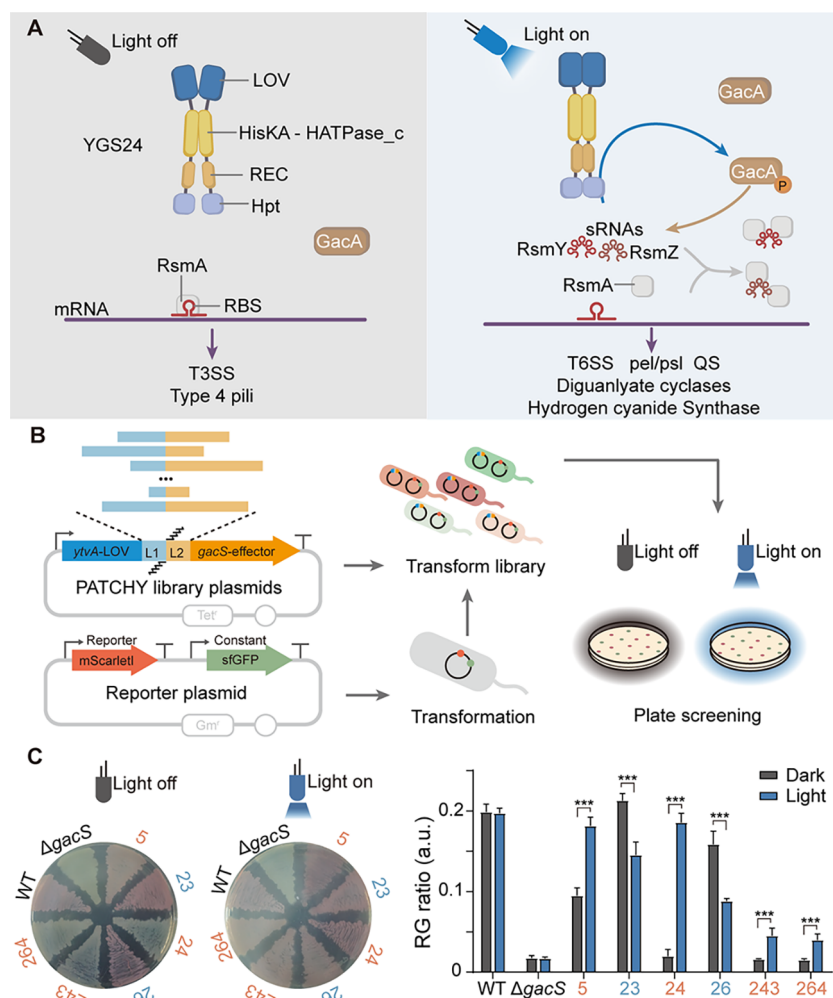


**Figure 1.** Development of the light-regulated YGSs. (A) Schematic representation of different states of the YGS/Rsm signaling cascade in light-off and light-on conditions. The chimeric YGS24 protein has a Nterminal LOV sensor domain, a catalytic core (comprising the HisKA and HATPase\_c domains), an REC domain, and a C-terminal Hpt domain. Under darkness (left), YGS24 has poor kinase activity to phosphorylate its cognate response regulator GacA, but under blue light (right) YGS24 can readily phosphorylate GacA probably because of structural changes. Free RsmA (gray box) binds to certain mRNAs, resulting in activating virulence factors associated with acute infections such as T3SS or type 4 pili. Phosphorylated GacA-activated transcription of the small RNAs (red coiled structures), RsmY and RsmZ, which sequester RsmA, thereby releasing the repression of chronic virulence relating to T6SS, polysaccharides such as Pel and Psl, QS, diguanylate cyclases, and hydrogen cyanide. T3SS, type 3 secretion system; T6SS, type 6 secretion system; Pel/Psl, two polysaccharides; QS, quorum sensing. (B) Construction and screening of the light-respondent YGSs. A library of plasmids within which are the YtvAGacS fusions with different truncation recombinants of entire linkers from the YtvA protein (L1) and GacS protein (L2) as linkers was generated. The library of plasmids was transformed to *gacS*\_PAO1 containing a fluorescence-based reporter plasmid for evaluating the transcription of *rsmY*. On the basis of the reporter plasmid, green fluorescence protein sfGFP is constantly expressed, while expression of the red fluorescent reporter mScarlet1 is promoted by active hybrids *via* phosphorylation of the response regulator GacA. Thereby, we could screen the YGSs by comparing the colony-fluorescence on the plates under darkness and blue light. (C) Images and bacteria colony RFP-to-GFP ratio (RG ratio) histogram of the LB plate assays of *rsmY* promoter response activity. Strains selected by screening were grown on LB agar supplemented with the appropriate antibiotics, either under darkness (left plate image) or under the illumination of blue light (right plate image) for 36 h (left images) or 32 h (right histogram). *P. aeruginosa* PAO1 wild type (WT) and *gacS*\_PAO1 mutant ( $\Delta gacS$ ) with empty vector were here as control groups. All of these strains contain the reporter plasmid described in panel B. Red colony (or high RG ratio) indicates higher transcription level of *rsmY* and higher net kinase activity of the hybrid protein than green colony (or low RG ratio). Red numbers, bacteria samples carried light-activated YGS proteins; blue numbers, bacteria samples carried light-inactivated YGS proteins.

spatiotemporal control of pathogenicity. The global Gac/Rsm regulatory cascade is of paramount importance for the regulation of lifestyles and the expression of virulence factors in various Gram-negative bacteria such as *Pseudomonas aeruginosa* (*P. aeruginosa*), a highly prevalent opportunistic human pathogen.<sup>7</sup> This regulatory network is based on a two-component system comprising the sensor kinase, GacS, and its response regulator, GacA, which could be activated through phosphorylation by GacS. The downstream regulator, RsmA,

an RNA-binding protein that regulates translation by binding to the 5' untranslated regions of certain mRNAs, is also a center to this regulatory network.<sup>8</sup> RsmA directly represses genes required for sessile lifestyle and chronic infections and has a positive effect on the expression of virulence factors associated with acute infections such as type 3 secretion system (T3SS) or type 4 pili.<sup>9,10</sup> When GacS responds to the environmental signals which remain elusive, its enzymatic activity of phosphorylating the response regulator GacA will be

modulated. Phosphorylated GacA activates the transcription of small RNAs, RsmY and RsmZ, which antagonize the regulatory activity of RsmA.<sup>11</sup> Each of RsmY and RsmZ has multiple RsmA-binding sites and function by sequestering RsmA from target mRNAs, thereby downregulating acute infection and upregulating genes involved in chronic virulence such as the type 6 secretion system (T6SS) and quorum sensing (QS).<sup>12,13</sup> Given that the two-component system (TCS) is the major upstream initiator of the Gac/Rsm cascade, we first sought to engineer a light-regulated histidine kinase optogenetic system based on GacS/GacA TCS in *P. aeruginosa* and thus optogenetically control its pathogenicity. Here, we reprogrammed the input signal specificity of GacS by replacing its input sensor domain, which confers unknown environmental sensitivity on its kinase activity, by the light-oxygen-voltage (LOV) blue light sensor domain of YtvA from *Bacillus subtilis*. A certain amount of the resulting fusion proteins retain kinase activity to activate the expression of sRNA, but are regulated by blue light instead of by other signals. We demonstrated and characterized one of the resultant fusion proteins named YGS24 that enabled the control of the Gac/Rsm regulatory signaling cascade in a light-dependent manner with low background activity and high light induction efficiency in *P. aeruginosa* (Figure 1A).

We then tested the light-inducing pathogenicity switch of *P. aeruginosa* cells *in vivo* in two different *Caenorhabditis elegans* (*C. elegans*) pathogenesis models, the slow-killing model and the lethal paralysis model. In the slow killing model, *P. aeruginosa* strain PA14 can kill *C. elegans* in an infection-like process within several days on minimal media (slow killing media, SK media) *via* colonization in the nematode intestinal lumen.<sup>14</sup> Another *P. aeruginosa* strain PAO1 can cause lethal paralysis of the nematode *via* cyanide poisoning when grown on rich media (brain–heart infusion media, BHI media).<sup>15,16</sup> In both pathogenesis systems, the irradiated engineered protein executed the inherent GacS histidine kinase activity involving the expression of infection virulence factors and the synthesis of cyanide, respectively, hence resulting in the enhanced capability to kill *C. elegans*. Furthermore, we activated the Gac/Rsm signaling cascade of cells present in the lumen of the *C. elegans* intestine by light and observed the lumen expansion due to colonization of PA14. Altogether, we regulated the infection signaling cascade of *P. aeruginosa* by an engineered light-responsive protein.

## RESULTS AND DISCUSSION

**Engineered Fusion Proteins YGSs Displaying Light-Dependent Kinase Activity in *P. aeruginosa*.** *B. subtilis* YtvA comprises an N-terminal LOV sensor domain adjacent to a C-terminal of sulfate transporter and AntiSigma factor antagonist (STAS) domain.<sup>17</sup> The two domains are connected by a short  $\alpha$ -helical linker (named J $\alpha$  helix).<sup>18</sup> After activation by blue light, the dark-adapted state of the LOV domain (D<sub>447</sub>) reaches the light-adapted state (S<sub>390</sub>) *via* a singlet excited state and a FMN triplet state within microseconds.<sup>19–21</sup> In the absence of blue light, the YtvA dark-adapted state recovers within 2600 s at room temperature, while recovery of the isolated LOV domain even takes more time.<sup>22</sup> YtvA dimerizes in a head-to-head fashion. J $\alpha$  helix relays the structural changes within the photosensor LOV module resulted from light absorption to alter the function of the effector STAS module.<sup>23</sup>

GacS is the sensor kinase of a TCS that globally regulates the expression of acute and chronic virulence factors in *P.*

*aeruginosa*.<sup>10,24</sup> The N-terminus of GacS contains two transmembrane regions. The cytoplasmic site of GacS contains an input domain; histidine kinases, adenylyl cyclases, methyl binding proteins, phosphatases (HAMP) domain; and three phosphotransfer domains: transmitter domain, receiver (REC) domain, and Hpt domain<sup>25</sup> (Figure 1A). The transmitter is made up of a HisKA domain and a HATPase-c domain. Upon receiving a stimulus through the input domain, the transmitter domain hydrolyzes ATP to ADP using the HATPase-c domain and autophosphorylates in the HisKA domain, then phosphorylates the REC domain which phosphorylates the Hpt domain.<sup>26</sup> The Hpt domain then transfers the phosphoryl group to the cognate response regulator GacA. Both GacS and GacA might also be active as dimers.<sup>7</sup>

We produced the light-regulated derivatives of GacS named YGSs by replacing the two transmembrane regions and the HAMP domain of GacS with the LOV domain of YtvA (Figure S1). Linkers play eminent roles in the construction of chimeric protein YGSs, given that they functionally conjoined the input module from YtvA and the phosphotransfer module from GacS. Consequently, we applied the Primer-Aided Truncation for the Creation of Hybrid Proteins (PATCHY) method<sup>27,28</sup> for efficient generation of the library of hybrid proteins that differ in length and composition of the linkers. The LOV domain of YtvA (amino acids 1–127) with the entire C-terminal linker segment (J $\alpha$  helix, here named L1, amino acids 128–147) and the phosphotransfer module (effector) of GacS (amino acids 283–925) with the N-terminal linker region (modeled to form a helical structure by Swiss Model, here named L2, amino acids 244–282) were seamlessly fused together to construct the original fusion YGS\_tmpl (Figure S1). The YGS\_tmpl, under the control of the native *gacS* promoter, was cloned into the plasmid pUCP20. This obtained plasmid functioned as the template plasmid. Unlike with the use of the classical PATCHY strategy, in which the template plasmids are removed in a final step by introducing a unique restriction site between L1 and L2,<sup>28</sup> we used nearly a negligible amount of template plasmids within which no restriction site was added between two linker segments in the following PCR (see methods). A forward or reverse set of primers was staggered in increments of single amino acids of the L1 or L2. The template plasmids were then amplified in a one-pot PCR reaction with two sets of primers to generate linker truncations. The resultant linearized fragments were self-circularized to produce the library. Strains were generated by introducing each of PATCHY library plasmids into the *gacS* deletion mutant of PAO1, a wild type of *P. aeruginosa*. These strains were named a series of RO1-YGSs, for example of which is RO1-YGS24 that represents the strain carrying YGS24. And to facilitate the library screening and subsequent analysis, we engineered and exploited the transcription reporter plasmid of *rsmY*,<sup>29</sup> one of the small RNAs that are directly activated by the TCS of GacS/GacA, as a proxy for YGS/GacA/Rsm activity, named RP1-mScarletI-sfGFP. In this reporter, an RNaseIII processing site is located between the *rsmY* promoter and the RBS of the *mScarletI* gene to ensure the independent translation of the reporter gene, and green fluorescent protein sfGFP is constitutively expressed. We introduced the reporter into RO1-YGSs cells. Accumulation expression of the fluorescent protein generates red colonies, indicating that transcription of *rsmY* is upregulated by activated hybrids protein *via* phosphorylation of GacA, while a colony that carries the hybrid with low net kinase activity remains

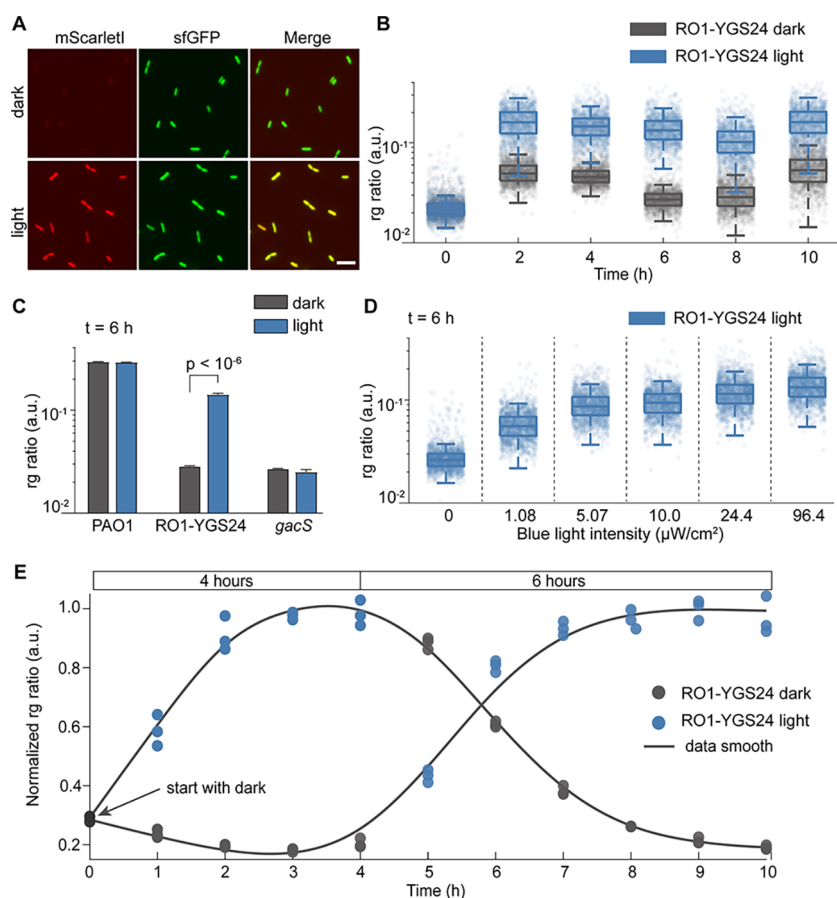


**Figure 2.** Performance of light-activated protein YGS24 in *gacS\_PAO1* mutant. Strains were transformed with a *rsmY* reporter encoding the mScarletI fluorescent protein. A *sfGFP* reporter fused to constitutive promoter J23102 served as an internal control. (A) The mScarletI, sfGFP, and corresponding merged fluorescence microscopy images of RO1-YGS24 under blue light (bottom) and darkness (top). Scale bar, 5  $\mu\text{m}$ . (B) Boxplot of rg ratio separated by cells illuminated with and without blue light. Every dot in the plot diagram represents one counted cell; more than 103 cells from three replicates were analyzed. (C) Rg ratio of wild type PAO1, RO1-YGS24, and *gacS\_PAO1* measured after 6 h under blue light or darkness. Data represent mean values of 103 single-cell events; error bars represent 1 SD of  $n = 3$  biologically independent samples. (D) Rg ratio of RO1-YGS24 measured after blue light illumination of different intensities for 6 h. (E) Rg ratio measured at indicated times during incubation with illumination under continuous blue light for 4 h and then by 6 h darkness, or with inverse illumination conditions. Every circle represents mean values of 103 single-cell events; data are representative of  $n = 3$  independent experiments.

green. We therefore screened the PATCHY libraries of YtvA-GacS fusions by color changes of colony appearance in the dark and light (Figure 1B). After winnowing about 384 colonies, six of these strains were found with obvious light-dependent *rsmY* reporter response activity, indicating the light-mediated kinase activity to regulate the expression of sRNA. We determined the nucleotide sequence of the corresponding YGSs by DNA sequencing (Figure S1). We showed that colonies of the cells that contain YGS23 or YGS26 faded upon blue light, reflecting light-inactivated kinase activity, and rest of the fusions, YGS5, YGS24, YGS243, and YGS264 displayed desired, light-activated kinase activity (Figure S1 and Figure 1C). We had a predilection for YGS24 due to its lower background activity and higher product of light-induced protein as judged by colony color and used it in all subsequent studies (Figure 1C).

**Characterization of Light-Induced YGS24 Activity in *P. aeruginosa*.** As describe above, we focused on YGS24. To further explore its light activated kinase activity in *P. aeruginosa*, we measured the activation of mScarletI transcriptional reporter for *rsmY* at the single-cell level as a ratio to a constitutively expressed *sfGFP* reporter in the cells of RO1-YGS24. We verified that the increase in the fluorescence ratio

of mScarletI-to-sfGFP (RFP-to-GFP ratio, RG ratio) was mainly a result of the increased activity of the *rsmY* promoter as opposed to the little changes in the sfGFP normalization control. Single cells have significant induced *rsmY* expression within 2 h under a constant 470 nm light of 96.4  $\mu\text{W}/\text{cm}^2$  (Figure 2A,B). The mean fluorescence intensity of cell populations of RO1-YGS24 in darkness remained at low level as did that of the *gacS* mutant, while the fluorescence level of cells under light was comparable with that of wild type PAO1 (Figure 2C and Figure S2). To determine the light intensity dependence of YGS24 activity, we measured the RG ratio for single cells in culture medium after illumination for 6 h with 470 nm of varying intensity. Even a light intensity of around 1  $\mu\text{W}/\text{cm}^2$  can partially activate, and an intensity of approximately 25  $\mu\text{W}/\text{cm}^2$  can completely activate, the blue light dependent *rsmY* expression (Figure 2D). Moreover, the YGS24-based optogenetical system was demonstrated to exhibit fully reversible activation of the Gac/Rsm signaling cascade (Figure 2E). Additionally, we noticed that the cells of RO1-YGS24 grown under darkness showed slightly faster growth than the cells exposed to light, and a similar growth defect was observed in wild type cells comparable to the cells of the *gacS* mutant, which indicated that growth inhibition

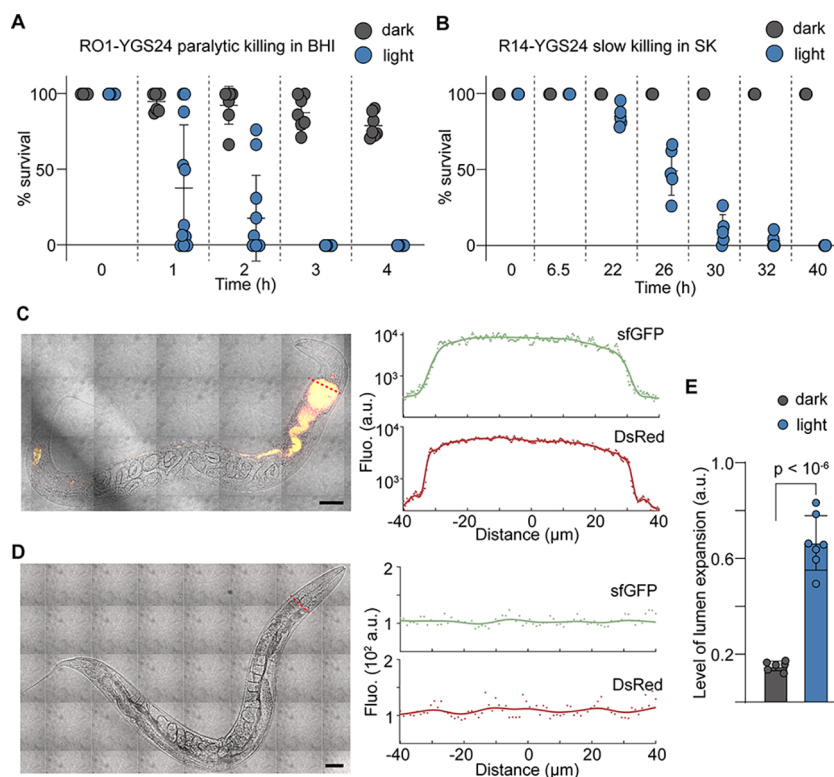


**Figure 3.** *P. aeruginosa*-*C. elegans* killing assays. (A) *C. elegans* survival assays comparison between the strain RO1-YGS24 or (B) R14-YGS24 with and without blue light. Every circle represents data of one biologically independent experiment. (C) The entire lumen of worms fed on illuminated cells of R14-YGS24-(RP2-sfGFP-DsRed.T3) for 20 h was filled with fluorescence-expressing cells. In contrast, (D) the lumen of worms fed on cells growing under darkness for the same time showed little detectable fluorescence. Scale bar, 50  $\mu\text{m}$ . Intensity graph was plotted as GFP and RFP intensities across the *C. elegans* intestine drawing with the red dotted line from left to right in both panels C and D. (E) The degree of the anterior intestine expansion of worms fed on R14-YGS24-(RP2-sfGFP-DsRed.T3) under continuous blue light was significantly higher than that of worms fed on cells under darkness. Data represent the mean  $\pm$  SD from seven biologically independent samples; every circle represents an individual data point from one worm.

correlated with the activation of the Gac/Rsm pathway, excluding the possibility that phototoxic effects are responsible for this phenomenon (Figure S3).

**Induction of Pathogenicity Switch of Cells through Blue Light in *P. aeruginosa*-*C. elegans* Models.** The Gac/Rsm pathway globally controls the expression of virulence factors in *P. aeruginosa*. For investigating the pathogenicity of *P. aeruginosa*, the nematode *C. elegans* has been chosen as an alternative host.

It has been shown that *P. aeruginosa* PAO1 kills *C. elegans* within 4 h when the strain is grown on rich brain–heart infusion (BHI) medium and *gacS* mutant is strongly attenuated in this virulence model.<sup>15,16</sup> To identify the virulence switch of RO1-YGS24 cells in the conditions of light and dark, we performed a paralytic killing assay with *C. elegans* as the pathogenesis system. In this assay, cells growing under constant 470 nm light of 120  $\mu\text{W}/\text{cm}^2$  killed up to 100% of the nematodes after 4 h, while cells growing in darkness killed only about 20% of total worms (Figure 3A).

For the other hand, when *C. elegans* is fed on *P. aeruginosa* PA14 grown on SK agar plate, the mechanism by which *P. aeruginosa* kills *C. elegans* involves an infection-like process that correlates with the accumulation of cells in the lumen of *C. elegans* intestine.<sup>14</sup> The killing occurs over the course of several days and is referred to as slow killing. Mutation in the *gacS* gene of PA14 was severely defective in the ability to kill *C. elegans* under slow-killing conditions.<sup>30</sup> We then constructed the strain named R14-YGS24, using a similar strategy with

RO1-YGS24 to replace the *gacS* naturally present in the wild type PA14 with the gene of YGS24, and examined whether light functions on our engineered cells in this killing model. We fed *C. elegans* on R14-YGS24 cells growing under the conditions of illumination and darkness, respectively. As the detailed statistics show in Figure 3B, the worms died within 20–40 h under illumination conditions, while no killing was observed during the experiment period in darkness, indicating that the unilluminated cells are nonpathogenic. We further confirmed that the cells that have the deletion of *gacS*, either in PAO1 or PA14, are seriously deficient in killing *C. elegans*, which are similar to the RO1-YGS24 or R14-YGS24 cells under darkness, while the lethality of the RO1-YGS24 or R14-YGS24 cells on *C. elegans* under light conditions are comparable with that of wild type cells (Figure S4). Taken together, these results showed that we had the ability to optogenetically regulate the virulence of *P. aeruginosa* cells ranging from the level of *gacS* mutant to wild type with the use of engineered photoresponsive protein YGS24.

To verify that light induced the signal pathways of *P. aeruginosa* we had already known in engineered cells, we designed a translational fusion reporter of *hcnB* in RO1-YGS24 and of *clpVI* in R14-YGS24 (*hcnB* associates with cyanide poisoning and *clpVI* is connected with infection virulence) as a proxy for the pathogenicity in its corresponding killing model<sup>31,32</sup> (for details see Methods). We showed that the illumination induction strongly boosted the expression of the cyanide poisoning marker *hcnB* in RO1-YGS24 and the

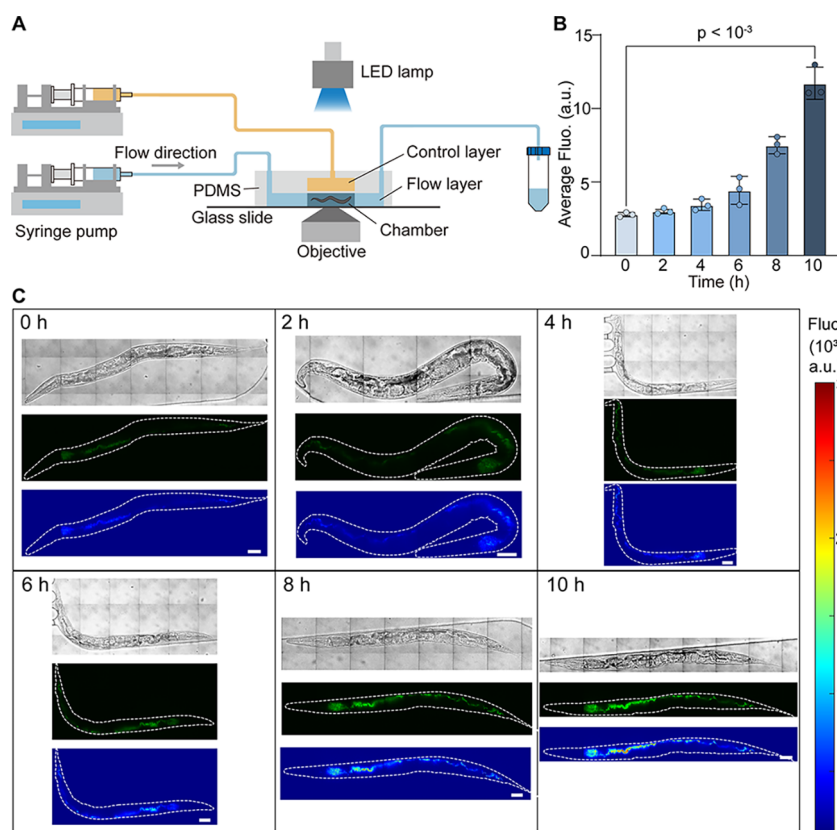


**Figure 4.** Light-induced infection process in *P. aeruginosa*–*C. elegans* model. (A) Schematic representation of experiment for activating YGS/Rsm signaling cascade of *P. aeruginosa* in *C. elegans* in the microfluidic device by blue light. (B) Cells accumulated over time in the lumen of *C. elegans* illuminated with blue light. Data represent the mean  $\pm$  SD from three biologically independent samples; every circle represents an individual data point from cells in one worm. (C) Bright-field (upper), sfGFP fluorescence (middle) microscopy images, and heat map for fluorescence intensity (lower) showed spatial control over blue-light induced gene expression from R14\_YGS24-(RP2-sfGFP-DsRed.T3) in the intestine of *C. elegans*. Used as a control group some worms fed on under the same condition and transferred to dark environment (Figure S7). Scale bar, 50  $\mu$ m.

chronic virulence marker *clpVI* in R14-YGS24 (Figure S5), in accordance with the results of killing assays.

To further monitor the living state of *C. elegans* during the infection process, we engineered the R14-YGS24 cells expressing sfGFP and DsRed.T3 to feed nematodes, in which DsRed.T3 was constitutively expressed for visualization of cells and sfGFP was used as the proxy for sRNA expression. After 20 h of feeding on illuminated cells, as shown in Figure 3C, both green and red fluorescence was observed throughout the expanded lumen of worm intestines, indicating the accumulation of cells with an activated Gac/Rsm cascade. In contrast, there are few cells present, indicated by very little fluorescence, in the lumen of worms fed on unilluminated cells at this time point (Figure 3C,D). The level of expansion of lumen of worms, which we roughly defined as the ratio of widths of the anterior intestine section of lumen to the body part of *C. elegans* at the measured time, stayed below 0.2 for the unilluminated ones, while it increased to  $0.68 \pm 0.1$  for the illuminated ones after 20 h feeding with R14-YGS24. (Figure 3E). Collectively, these results suggested that the light induced activation of the Gac/Rsm cascade of PA14 cells had the ability to accumulate in the worm gut accompanied by lumen expansion gradually, thereby resulting in the lethal infection.

**Regulation of *P. aeruginosa* Gac/Rsm Cascade in *C. elegans* In Situ.** As chemically induced systems are subject to complex pharmacokinetics, poorly controlled diffusion, and difficulties in removing inducers, we sought to use the light-activated system to activate the infection cascade of bacterial

cells in the intestine of *C. elegans*. We performed it using the PA14-*C. elegans* slow-killing model mentioned above to ensure a sufficient induction time before the worm died. Given that the unilluminated engineered cells are nonpathogenic and barely replicate in the worm intestine, we mixed wild type cells to help the engineered cells to colonize in the worm gut. We fed *C. elegans* on the mixed cells under darkness for 25 h and transferred the worms to a microfluidic device<sup>33</sup> (Figure 4A and Figure S6) for spatial light induction (for details see methods). We monitored the cells with intermittent microscopy imaging. After illumination for 2 h, green fluorescence was observed within the illuminated worms, indicating the induced expression of sRNA and the expression switch of downstream genes of the Gac/Rsm pathway (Figure 4B, C). Following illumination to 10 h, green fluorescence increased more than 3-fold (Figure 4B,C). In contrast, the green fluorescence barely changed in unilluminated worms (Figure S7). At this time point, we noticed that the worms, both under darkness and illumination condition, had an expansion of lumen and became immobile, and this might be mainly caused by the continued virulence of wild type cells from mixture feeding.

Light offers a more precise, efficient, and reversible way to manipulate biological functions directly at the protein level. In the present study, we constructed the photoreceptor YGSs by recombining the blue light responsive LOV photosensor module of *B. subtilis* YtvA with the *P. aeruginosa* GacS histidine kinase effector (Figure 1A and Figure S1).

Optogenetic protein interaction switches employ conformational changes of specific proteins, such as LOV domain proteins, to control protein–protein interactions by light.<sup>34</sup> However, the applications of optogenetics have mainly been in eukaryotic cells,<sup>35</sup> and these photoresponsive proteins designed in bacteria were mainly in model strain such as *Escherichia coli* to enable spatiotemporally transcriptional activation of user-defined exogenous or endogenous genes from a specific promoter under light illumination and could be further used to manipulate many biological processes.<sup>36–38</sup> Nevertheless, adoption of the transgene systems to other species of bacteria may introduce interference with endogenous proteins or genes due to homology.<sup>39,40</sup> These light-switchable gene expression systems, most importantly, are incapable of regulating global regulatory cascades partly because of large numbers of downstream genes, which severely restricts the utilization of such optogenetic systems for further systemic research that involves complex genetic regulation such as pathogenicity.

The resultant protein YGS24 showed light-dependent kinase activity of GacS, thus allowing us to reversibly stimulate the global Gac/Rsm signaling cascade which is of central importance for the regulation of infection and virulence factors in *P. aeruginosa* by blue light (Figure 1C and Figure 2). However, poor penetration of blue light through non-transparent tissues should be considered for further use in the research of cell cultures or animal models. The insights that emerged from YGSs engineering are expected to facilitate engineering of new light-activated optogenetic tools, fusing a photosensory module that encompassed the spectral region needed and a sensor kinase of TCSs.

When tested in host models, our engineered optogenetic system enabled the light-regulated pathogenicity switch of bacterial cells and correspondingly tuned the susceptibility of *C. elegans* to *P. aeruginosa*-mediated killing (Figure 3). In the two *P. aeruginosa*–*C. elegans* models, unilluminated strains RO1-YGS24 and R14-YGS24 were incapable of killing *C. elegans*, namely, the light induced innocuous-to-mortal virulence switch of the pathogen. We expected to control the analogous morbidity switch in various environments or hosts, as the Gac/Rsm cascade in *P. aeruginosa* and other Gram-negative bacteria regulated different phases of pathogenicity. The absence of GacS of clinical *P. aeruginosa* decomposed the Gac/Rsm pathway leading to depletion of the sRNAs RsmY/RsmZ and, in consequence, to expression of the type 3 secretion system (T3SS) or type 4 pili, the hallmark of acute infection, while switching off the expression of virulence factors promoting chronic infection such as T6SS, hydrogen cyanide synthase, or Pel polysaccharides<sup>10</sup> (Figure 1A). This suggested that we might control the acute-to-chronic virulence switch in *P. aeruginosa* by blue light.

*P. aeruginosa* PA14 kills *C. elegans* involving a chronic infection-like process that is associated with the colonization and accumulation of cells in the lumen of the *C. elegans* intestine in SK medium.<sup>14</sup> Because of minimal adherence of the strain R14-YGS24-(RP2-sfGFP-DsRed.T3) in the lumen of *C. elegans* intestine under the dark condition, we fed worms on commingled cells of R14-YGS24-(RP2-sfGFP-DsRed.T3) and PA14 and induced the innocuous-to-mortal virulence switch of *P. aeruginosa* by blue light. Because of the restless of worms, they were temporally immobilized by the microfluid device for less than 1 min, and lacking in efficient tracking approach such as a technology with higher spatial resolution of 10  $\mu\text{m}$  for optogenetically stimulating specific parts of body in freely

behaving *C. elegans*,<sup>41</sup> we regulated the accumulation of cells within the whole worm, instead of in the part of lumen of one worm or at single-cell revolution theoretically. Furthermore, we introduced additional PA14 to help R14-YGS24 accumulation in the *C. elegans* lumen of the intestine. By comparison, it will be more meaningful and promising to introduce only R14-YGS24 by partially inducing the pathogenicity and ability of colonization before induction into the microfluidic chip using appropriate low blue-light intensity. The next step could be establishing the corresponding relationship between the blue light intensity and the colonization ability of the bacteria in the worm intestine.

Host–pathogen interactions can be investigated on many levels, considering that not all interactions lead to disease and those that do have a complex progression that heads to this state. Moreover, the genetic uniqueness and diversity of each host or pathogen and the inherent variability in the complexity and types of host–pathogen interactions result in an immense and somehow unfathomable array of different combinations. Each individual host–pathogen interaction relationship is unique, and the pathogen would show different attributes of aggressiveness and toxicity to various tissues even within one host.<sup>42</sup> Overall, we engineered a new light-activated protein to optically control the infection and virulence factors in *P. aeruginosa*, thereby further expanding the tool set in the area of pathogenic research that has great demands for precise spatiotemporal control of bacterial pathogenicity.

## MATERIALS AND METHODS

**Microbiological Methods.** The plasmids, strains, and primers used in this study are listed in Tables S1–S3 in the Supporting Information, respectively. Standard molecular cloning techniques were used for construction of related plasmids in *E. coli* strain Top10. Deletion mutants *gacS*\_{PAO1} and *gacS*\_{PA14} were constructed by using well-established protocols for *P. aeruginosa* based on two-step allelic exchange.<sup>43</sup> To screen the library and test the performance of YGS24, we exploited the transcriptional reporter of *rsmY*, named RP1-mScarletI-sfGFP. To construct this reporter plasmid, PCR fragments, promoter *PrsmY*, an RNaseIII processing site, red fluorescent protein *mScarletI*, and terminators (TOT1) were assembled into one piece by overlap extension PCR.<sup>44</sup> Another fragment J23102-*sfGFP*-TOT1 was aligned by the same way. After the overlap PCR, the two resulting aligned fragments were then cloned into pJN105 through multiple cloning sites. The *hcnB* translational reporter HP-mScarletI-sfGFP and *clpVI* translational reporter CP-mScarletI-sfGFP were constructed by replacing *PrsmY*-RNaseIII with translational promoter *PhcnB* and *PclpVI*, respectively. To visualize bacteria more clearly in the intestine of *C. elegans*, we construct another reporter RP2-sfGFP-DsRed.T3 by replacing *mScarletI* and *sfGFP* with *sfGFP* and *dsRed.T3*, respectively, using PCR and Gibson assembly.<sup>45</sup> All PCR reactions here were performed with a high-fidelity polymerase (Phanta Super-Fidelity DNA Polymerase, Vazyme). Unless performing *C. elegans* assays, both *E. coli* and *P. aeruginosa* strains were grown in LB medium or on LB agar. Plasmids were maintained in media supplemented with the following concentrations: gentamicin (Aladdin) 15  $\mu\text{g}/\text{mL}$  (pJN105, pUCP20Gm and derivatives), tetracycline (Aladdin) 10  $\mu\text{g}/\text{mL}$  (pUCP20Tet and derivatives) in *E. coli*; gentamicin 30  $\mu\text{g}/\text{mL}$  (pJN105, pUCP20Gm and derivatives), tetracycline 100  $\mu\text{g}/\text{mL}$  (pUCP20Tet and derivatives) in *P. aeruginosa*. *C.*

*C. elegans* N2 strain was kindly shared by the lab of Shouhong Guang (University of Science and Technology of China), and was grown on *E. coli* (OP50) lawns on nematode growth media agar (NGM) at 20 °C. To obtain a synchronized population, gravid adult nematodes were transferred by wire pick to fresh NGM plates with OP50 for 2–4 h to lay eggs, and then removed.

Cells of RP1-mScarletI-sfGFP were used for YGS24 light-sensitive assay. Strains were streaked on LB agar from frozen stocks and incubated overnight at 37 °C. A single colony was inoculated with a 1 mL culture of LB broth in the dark at 30 °C until OD600 reached approximately 2.4. The culture was diluted to an OD600 of approximately 0.05 and incubated under blue light or in the dark at 30 °C/250 rpm. Fluorescence intensities were measured every 2 h. Growth curves were measured under the same condition giving an initial diluted OD600 of ~0.02. The translational reporter HP-mScarletI-sfGFP and CP-mScarletI-sfGFP were transformed into RO1-YGS24 and R14-YGS24, respectively. The two strains were cultured overnight followed by 1:100 dilution to 1 mL BHI or LB medium and cultured for 14 h (RO1-YGS24-(HP-mScarletI-sfGFP)) or 11 h (R14-YGS24-(CP-mScarletI-sfGFP)) at 30 °C/250 rpm under blue light or darkness, and then fluorescence intensities were measured. For the intensity curves measurement, the light condition was changed from blue light to dark, or on the contrary. The overnight strain culture was diluted to an OD600 of ~0.05 and then incubated in a shaker with 250 rpm at 30 °C in the dark until OD600 reached approximately 0.6. The culture was then diluted to an OD600 of ~0.3 and incubated in the shaker under certain light conditions. Every hour, the strain culture was diluted to an OD600 of ~0.3 and the fluorescence intensity was measured.

For PATCHY library screening, Petri dishes were placed under 3 W/m<sup>2</sup> blue light emitting from an LED lamp ( $\lambda = 470$  nm, M470L2, Thorlabs) or in the dark. For *C. elegans* assays, blue light intensity from LED was set at approximately 1.2 W/m<sup>2</sup>.

**PATCHY Library.** The PATCHY library was generated by using a modified version of the published protocol.<sup>27</sup> The *BsYtvA*-LOV domain and the three phosphotransfer domains from *PaGacS* with their full-length linkers (*BsYtvA* residues 1–147, *PaGacS* residues 244–925) were cloned in tandem in the pUCP20, and the tandem fusion was named YGS\_tmpl (Figure S1). This constructing plasmid, denoted pUCP20-YGS\_tmpl, was functioned as the template. The reserve (Patchy-F from 1 to 21) and forward (Patchy-R from 1 to 40) primers were staggered by increments of nucleotide triplets and annealed to different positions within the C-terminal LOV module linker L1 and the linker of the N-terminal phosphotransfer domains termed L2, respectively. A one-pot PCR reaction with two sets of forward and reserve primers was carried out to amplify the template. To reduce the template in the PCR products, we reduced the dosage of the template to 0.002 ng/ $\mu$ L in the PCR reaction. The PCR products were purified by PCR-clean up (AxyPrep PCR Cleanup Kit, Axygen) and then self-circularized *via* T4 Polynucleotide Kinase (ThermoFisher), ATP (ThermoFisher), and T4 DNA Ligase (ThermoFisher). The reaction mix was transformed into chemically competent *E. coli* Top10. The plasmids were extracted and transformed into PAO1 with pJN105-*PrsmY* reporter (RP1-mScarletI-sfGFP). Cells harboring the construct and the reporter were grown in LB medium with tetracycline (100  $\mu$ g/mL) and gentamicin (30  $\mu$ g/mL) for 20 h at 37 °C.

Single colonies were then inoculated in 96-deep-well plates containing 600  $\mu$ L of LB (with tetracycline and gentamicin) per well for 20 h at 37 °C. A 2  $\mu$ L aliquot of each single colony solution was grown on LB medium (with tetracycline and gentamicin) at 30 °C under blue light and in the dark to screen effective fusions. With one forward primer for each amino acid in L2 (39 residues) and one reverse primer for each amino acid in L1 (20 residues), 61 primers are theoretically capable of generating  $40 \times 21 = 840$  fusion variants. However, we obtained and screened about 384 colonies in the experiment.

**Paralytic Killing Assay.** *P. aeruginosa* strains were incubated in the shaker with 250 rpm at 37 °C overnight in brain–heart infusion (BHI) (Oxoid) broth and then diluted 100-fold into fresh broth. BHI agar plates (60 mm diameter) were spread with 200  $\mu$ L of each of the dilutions and then incubated for 24 h at 37 °C to form bacteria lawns. Gentamicin was added at 30  $\mu$ g/mL if required. Adult nematodes from stock plates were collected in a minimal volume of M9 buffer (22 mM KH<sub>2</sub>PO<sub>4</sub>, 42 mM Na<sub>2</sub>HPO<sub>4</sub>, 86 mM NaCl, 1 mM MgSO<sub>4</sub>). Droplets containing nematodes were spotted onto the *P. aeruginosa* lawns. The plates were then sealed with parafilm and incubated at room temperature. The paralysis of the nematodes was scored with a microscope. The assays of RO1-YGS24 strain with gentamicin resistance were always under blue light or in the dark during the whole experiments. Each plate was scored at only one time point; we prepared the same plates for different time points at each experiment.

**Slow Killing Assay.** The slow killing assay was performed by using a modified protocol of previously described methods.<sup>14,46</sup> A 50  $\mu$ L aliquot of overnight cultures of *P. aeruginosa* strains (wild-type PA14, *gacS*\_PA14, R14-YGS24) was pipetted onto 60 mm diameter modified SK agar plates (tryptone instead of peptone was used) with or without 50  $\mu$ g/mL tetracycline, and was spread by using sterile L spreaders to entirely cover the plates. The plates were incubated at 37 °C for 24 h and then set at 25 °C for an additional 24 h. Synchronized adult worms were seeded on plates. The killing plates were incubated at 25 °C and scored for live worms at intervals. The assays of R14-YGS24 were performed under blue light and dark conditions, respectively.

**Microfluidic Experiment.** The microfluidic chip was designed to enable individual worm loading, long-term culture, harmless immobilization, and fluorescence imaging. The chip was fabricated in PDMS (poly(dimethylsiloxane)), which is gas permeable, transparent, nonfluorescent, and biocompatible with organisms. The chip was composed of three layers: top control layer, middle PDMS membrane, and bottom flow layer (Figure S6). The bottom flow layer consisted of worm inlet, loading channels, and eight chambers (2 mm length, 500  $\mu$ m width, and ~60  $\mu$ m height) for worm culture and imaging. The captured worm was prevented from escaping due to the narrow grooves (50  $\mu$ m width, 20  $\mu$ m interval distance) at the end of chamber. The deformable PDMS membrane was assembled between the bottom flow layer and top control layer. By activating the microvalve in the control layer, the PDMS membrane deformed to the chamber in the flow layer and worms could be immobilized.

To observe bacteria behavior *in vivo*, a cell mixture comprising 40  $\mu$ L of overnight culture of PA14 harboring pJN105 and pUCP20Tet empty vectors and 10  $\mu$ L of overnight culture of R14-YGS24 carrying RP2-sfGFP-DsRed.T3 was cultured in darkness to prepare a bacteria lawn. Synchronized young-adult worms were fed for 25 h in



darkness and washed with M9 buffer to wipe off bacteria. Fresh M9 buffer containing worms was added into the inlets in the flow channel of the microfluidic device. After worms swam into the loading channel, they were loaded into the culture chambers under the M9 flow driven by syringe pump, and the device was placed in blue light. For imaging, worms were immobilized by controlling the microvalve in the control layer. To immobilize worms, the valve was switched on by positive pressure of water from the control layer. Then the deformable PDMS membrane was pushed up, to squeeze the worms to the side of the imaging channels so that worms could be immobilized and imaged. After imaging, the valve was switched off by removing pressure and then the worms could be released and recover their mobile activity quickly.

**Microscopy.** In colonies imaging assay, the fluorescent images were collected by a microzoom fluorescence microscope (Olympus, MVX10) equipped with a 1× objective (NA = 0.25) and a sCMOS camera (Photometrics, Prime BSI). GFP (sfGFP) or RFP (mScarlet) was excited using a 488 or 565 nm LED lights (Lumencor, Spectra X) and imaged using single-band emission filters (Semrock), GFP (520/28 nm) or RFP (598/25 nm).

In light-sensitive experiments, fluorescent images were collected by using an inverted fluorescent microscope (Olympus, IX71) equipped with a 100× oil immersion objective and two sCMOS cameras (Zyla 4.2, Andor). The GFP (sfGFP) and RFP (mScarletI) were excited by using 488/10 nm and 567/15 nm lasers respectively and the emission filters used were 520/28 nm and 631/36 nm, respectively. For the fluorescent intensity curves measurement, fluorescence imaging was performed using a spinning-disk confocal (CSU-X1; Yokogawa) inverted microscope (IX81; Olympus) equipped with a laser combiner system (Andor Technology), a 100× oil immersion objective (Olympus), and EMCCD camera (iXon897). To collect the fluorescence of sfGFP, a 488 nm laser was used as exciter, a 524/40 nm channel was used as emitter. The mScarletI was excited using a 561 nm laser and the fluorescence was detected by a 605/40 nm channel.

In *C. elegans* imaging assays, bacteria lawns were prepared by the same method in slow killing assays. Age-synchronized young-adult worms were collected for each experiment. Nematodes were fed with illuminated and unilluminated bacteria lawns of R14-YGS24 carrying RP2-sfGFP-DsRed.T3 for 20 h in light and darkness, respectively. To observe bacteria behavior *in vivo*, a mixture containing 40  $\mu$ L of overnight culture of PA14 carrying pJN105 and pUCP20Tet and 10  $\mu$ L of overnight culture of R14-YGS24 carrying RP2-sfGFP-DsRed.T3 was cultured in darkness to prepare a bacteria lawn. Worms were fed for 25 h in darkness and washed with M9 buffer to wipe off bacteria. The M9 buffer containing worms was added into an EP tube or microfluidic device and placed in blue light or darkness for 10 h. Images were collected using a spinning disk confocal inverted microscope as previously mentioned, a 60× oil immersion objective, and an EMCCD camera (iXon 897). The sfGFP or DsRed.T3 fluorescence was excited using a 488 or 561 nm laser, respectively, and imaged with two different emission channels (524 or 605 nm).

**Statistical Analysis.** Images acquired were analyzed using ImageJ software or MATLAB codes.<sup>47</sup> Cell masks were obtained using images of fluorescent protein which was driven by J23102, and then the reporter FP fluorescence was measured by computing the mean intensity within masks. To

obtain mean fluorescence intensity, we subtracted the average fluorescence intensity per pixel of the background from the average intensity per pixel in the given cell. Mean values and standard deviations were obtained from at least three independent experiments (biological replicates). Statistical analysis was performed with Student's *t* test using GraphPad Prism version 8.0.

## ■ ASSOCIATED CONTENT

### SI Supporting Information

The Supporting Information is available free of charge at <https://pubs.acs.org/doi/10.1021/acssynbio.1c00075>.

Lists of plasmids, strains, nematodes, and primers used in this study; alignment of linker regions of light-regulated YtvA-GacS fusions from PATCHY libraries; mean fluorescence intensity of cell populations under blue light; activation of the GacS leads to reduced growth; *P. aeruginosa*-*C. elegans* nematode model; light induced corresponding signal pathways of *P. aeruginosa* in engineered cells; schematic of the microfluidic device; microscope images of worms fed on mixture cells (PDF)

## ■ AUTHOR INFORMATION

### Corresponding Authors

**Fan Jin** – CAS Key Laboratory of Quantitative Engineering Biology, Shenzhen Institute of Synthetic Biology, Shenzhen Institutes of Advanced Technology, Chinese Academy of Sciences, Shenzhen 518055, China; Hefei National Laboratory for Physical Sciences at the Microscale; Department of Polymer Science and Engineering, University of Science and Technology of China, Hefei 230026, China; [orcid.org/0000-0003-2313-0388](https://orcid.org/0000-0003-2313-0388); Phone: +86 0755-26409621; Email: [fan.jin@siat.ac.cn](mailto:fan.jin@siat.ac.cn)

**Shuai Yang** – CAS Key Laboratory of Quantitative Engineering Biology, Shenzhen Institute of Synthetic Biology, Shenzhen Institutes of Advanced Technology, Chinese Academy of Sciences, Shenzhen 518055, China; Hefei National Laboratory for Physical Sciences at the Microscale; Department of Polymer Science and Engineering, University of Science and Technology of China, Hefei 230026, China; [orcid.org/0000-0001-8325-4994](https://orcid.org/0000-0001-8325-4994); Phone: +86 0755-26409621; Email: [yssamber@mail.ustc.edu.cn](mailto:yssamber@mail.ustc.edu.cn)

### Authors

**Xinyi Cheng** – Hefei National Laboratory for Physical Sciences at the Microscale; Department of Polymer Science and Engineering, University of Science and Technology of China, Hefei 230026, China

**Lu Pu** – CAS Key Laboratory of Quantitative Engineering Biology, Shenzhen Institute of Synthetic Biology, Shenzhen Institutes of Advanced Technology, Chinese Academy of Sciences, Shenzhen 518055, China

**Shengwei Fu** – Hefei National Laboratory for Physical Sciences at the Microscale; Department of Polymer Science and Engineering, University of Science and Technology of China, Hefei 230026, China

**Aiguo Xia** – CAS Key Laboratory of Quantitative Engineering Biology, Shenzhen Institute of Synthetic Biology, Shenzhen Institutes of Advanced Technology, Chinese Academy of Sciences, Shenzhen 518055, China

**Shuqiang Huang** – CAS Key Laboratory of Quantitative Engineering Biology, Shenzhen Institute of Synthetic Biology,

Shenzhen Institutes of Advanced Technology, Chinese Academy of Sciences, Shenzhen 518055, China

Lei Ni – CAS Key Laboratory of Quantitative Engineering Biology, Shenzhen Institute of Synthetic Biology, Shenzhen Institutes of Advanced Technology, Chinese Academy of Sciences, Shenzhen 518055, China

Xiaochen Xing – CAS Key Laboratory of Quantitative Engineering Biology, Shenzhen Institute of Synthetic Biology, Shenzhen Institutes of Advanced Technology, Chinese Academy of Sciences, Shenzhen 518055, China

Complete contact information is available at:

<https://pubs.acs.org/10.1021/acssynbio.1c00075>

## Author Contributions

<sup>#</sup>X.C., L.P., and S.F. contributed equally to this work. X.C., L.P., S.Y., and F.J. designed the project; X.C., L.P., and S.F. carried out the experiments and participated in data analysis; S.H. designed and provided the microfluidic devices; A.X., L.N., and X.X. contributed the microscopy methodology; S.Y. performed the majority of data analysis; X.C., L.P., and S.Y. wrote the manuscript.

## Notes

The authors declare no competing financial interest.

## ACKNOWLEDGMENTS

We thank professor Shouhong Guang of University of Science and Technology of China for gifting us *C. elegans* N2. This work was supported by National Key Research and Development Program of China (Grant No. 2020YFA0906900 and Grant No. 2018YFA0902700 to F.J.) and National Natural Science Foundation of China (Grant No. 31901028 to S.Y., Grant No. 21774117 to F.J., Grant No. 31700745 to X.X. and Grant No. 31700087 to L.N.) and China Postdoctoral Science Foundation (Grant No. 2020M672881 to S.Y.).

## REFERENCES

- (1) Casadevall, A., and Pirofski, L. A. (1999) Host-pathogen interactions: redefining the basic concepts of virulence and pathogenicity. *Infect. Immun.* 67 (8), 3703–3713.
- (2) Casadevall, A., and Pirofski, L. A. (2000) Host-pathogen interactions: basic concepts of microbial commensalism, colonization, infection, and disease. *Infect. Immun.* 68 (12), 6511–6518.
- (3) Moy, T. I., Ball, A. R., Anklesaria, Z., Casadei, G., Lewis, K., and Ausubel, F. M. (2006) Identification of novel antimicrobials using a live-animal infection model. *Proc. Natl. Acad. Sci. U. S. A.* 103 (27), 10414–10419.
- (4) Shan, Y., Fang, C., Cheng, C., Wang, Y., Peng, J., and Fang, W. (2015) Immersion infection of germ-free zebrafish with *Listeria monocytogenes* induces transient expression of innate immune response genes. *Front. Microbiol.* 6, 373.
- (5) Nehme, N. T., Liégeois, S., Kele, B., Giammarinaro, P., Pradel, E., Hoffmann, J. A., Ewbank, J. J., and Ferrandon, D. (2007) A model of bacterial intestinal infections in *Drosophila melanogaster*. *PLoS Pathog.* 3 (11), e173.
- (6) Toettcher, J. E., Voigt, C. A., Weiner, O. D., and Lim, W. A. (2011) The promise of optogenetics in cell biology: interrogating molecular circuits in space and time. *Nat. Methods* 8 (1), 35–38.
- (7) Heeb, S., and Haas, D. (2001) Regulatory roles of the GacS/GacA two-component system in plant-associated and other gram-negative bacteria. *Mol. Plant-Microbe Interact.* 14 (12), 1351–1363.
- (8) Brencic, A., and Lory, S. (2009) Determination of the regulon and identification of novel mRNA targets of *Pseudomonas aeruginosa* RsmA. *Mol. Microbiol.* 72 (3), 612–632.
- (9) Pessi, G., Williams, F., Hindle, Z., Heurlier, K., Holden, M. T., Cámara, M., Haas, D., and Williams, P. (2001) The global

posttranscriptional regulator RsmA modulates production of virulence determinants and N-acylhomoserine lactones in *Pseudomonas aeruginosa*. *J. Bacteriol.* 183 (22), 6676–6683.

(10) Goodman, A. L., Kulasekara, B., Rietsch, A., Boyd, D., Smith, R. S., and Lory, S. (2004) A signaling network reciprocally regulates genes associated with acute infection and chronic persistence in *Pseudomonas aeruginosa*. *Dev. Cell* 7 (5), 745–754.

(11) Brencic, A., McFarland, K. A., McManus, H. R., Castang, S., Mogno, I., Dove, S. L., and Lory, S. (2009) The GacS/GacA signal transduction system of *Pseudomonas aeruginosa* acts exclusively through its control over the transcription of the RsmY and RsmZ regulatory small RNAs. *Mol. Microbiol.* 73 (3), 434–445.

(12) Reimmann, C., Beyeler, M., Latifi, A., Winteler, H., Foglino, M., Lazdunski, A., and Haas, D. (1997) The global activator GacA of *Pseudomonas aeruginosa* PAO positively controls the production of the autoinducer N-butyl-homoserine lactone and the formation of the virulence factors pyocyanin, cyanide, and lipase. *Mol. Microbiol.* 24 (2), 309–319.

(13) Parkins, M. D., Ceri, H., and Storey, D. G. (2001) *Pseudomonas aeruginosa* GacA, a factor in multihost virulence, is also essential for biofilm formation. *Mol. Microbiol.* 40 (5), 1215–1226.

(14) Tan, M. W., Mahajan-Miklos, S., and Ausubel, F. M. (1999) Killing of *Caenorhabditis elegans* by *Pseudomonas aeruginosa* used to model mammalian bacterial pathogenesis. *Proc. Natl. Acad. Sci. U. S. A.* 96 (2), 715–720.

(15) Darby, C., Cosma, C. L., Thomas, J. H., and Manoil, C. (1999) Lethal paralysis of *Caenorhabditis elegans* by *Pseudomonas aeruginosa*. *Proc. Natl. Acad. Sci. U. S. A.* 96 (26), 15202–15207.

(16) Gallagher, L. A., and Manoil, C. (2001) *Pseudomonas aeruginosa* PAO1 kills *Caenorhabditis elegans* by cyanide poisoning. *J. Bacteriol.* 183 (21), 6207–6214.

(17) Aravind, L., and Koonin, E. V. (2000) The STAS domain - a link between anion transporters and antisigma-factor antagonists. *Curr. Biol.* 10 (2), R53–R55.

(18) Losi, A., Polverini, E., Quest, B., and Gärtner, W. (2002) First evidence for phototropin-related blue-light receptors in prokaryotes. *Biophys. J.* 82 (5), 2627–2634.

(19) Swartz, T. E., Corchnoy, S. B., Christie, J. M., Lewis, J. W., Szundi, I., Briggs, W. R., and Bogomolni, R. A. (2001) The photocycle of a flavin-binding domain of the blue light photoreceptor phototropin. *J. Biol. Chem.* 276 (39), 36493–36500.

(20) Salomon, M., Christie, J. M., Knieb, E., Lempert, U., and Briggs, W. R. (2000) Photochemical and mutational analysis of the FMN-binding domains of the plant blue light receptor, phototropin. *Biochemistry* 39 (31), 9401–9410.

(21) Song, S. H., Madsen, D., van der Steen, J. B., Pullman, R., Freer, L. H., Hellingwerf, K. J., and Larsen, D. S. (2013) Primary photochemistry of the dark- and light-adapted states of the YtvA protein from *Bacillus subtilis*. *Biochemistry* 52 (45), 7951–7963.

(22) Losi, A., Quest, B., and Gärtner, W. (2003) Listening to the blue: the time-resolved thermodynamics of the bacterial blue-light receptor YtvA and its isolated LOV domain. *Photochem. Photobiol. Sci.* 2 (7), 759–766.

(23) Möglich, A., and Moffat, K. (2007) Structural basis for light-dependent signaling in the dimeric LOV domain of the photosensor YtvA. *J. Mol. Biol.* 373 (1), 112–126.

(24) Goodman, A. L., Merighi, M., Hyodo, M., Ventre, I., Filloux, A., and Lory, S. (2009) Direct interaction between sensor kinase proteins mediates acute and chronic disease phenotypes in a bacterial pathogen. *Genes Dev.* 23 (2), 249–259.

(25) Rodrigue, A., Quentin, Y., Lazdunski, A., Méjean, V., and Foglino, M. (2000) Two-component systems in *Pseudomonas aeruginosa*: why so many? *Trends Microbiol.* 8 (11), 498–504.

(26) Whitworth, D. E., and Cock, P. J. A. (2009) Evolution of prokaryotic two-component systems: insights from comparative genomics. *Amino Acids* 37 (3), 459–466.

- (27) Stabel, R., Stüven, B., Ohlendorf, R., and Möglich, A. (2017) Primer-Aided truncation for the creation of hybrid proteins. *Methods Mol. Biol.* 1596, 287–304.
- (28) Ohlendorf, R., Schumacher, C. H., Richter, F., and Möglich, A. (2016) Library-Aided Probing of Linker Determinants in Hybrid Photoreceptors. *ACS Synth. Biol.* 5 (10), 1117–1126.
- (29) Yang, S., Cheng, X., Jin, Z., Xia, A., Ni, L., Zhang, R., and Jin, F. (2018) Differential production of Psl in planktonic cells leads to two distinctive attachment phenotypes in *Pseudomonas aeruginosa*. *Appl. Environ. Microbiol.* 84 (14), e00700–e00718.
- (30) Tan, M. W., Rahme, L. G., Sternberg, J. A., Tompkins, R. G., and Ausubel, F. M. (1999) *Pseudomonas aeruginosa* killing of *Caenorhabditis elegans* used to identify *P. aeruginosa* virulence factors. *Proc. Natl. Acad. Sci. U. S. A.* 96 (5), 2408–2413.
- (31) Bönemann, G., Pietrosiuk, A., Diemand, A., Zentgraf, H., and Mogk, A. (2009) Remodelling of VipA/VipB tubules by ClpV-mediated threading is crucial for type VI protein secretion. *EMBO J.* 28 (4), 315–325.
- (32) Laville, J., Blumer, C., Von Schroetter, C., Gaia, V., Défago, G., Keel, C., and Haas, D. (1998) Characterization of the hcnABC gene cluster encoding hydrogen cyanide synthase and anaerobic regulation by ANR in the strictly aerobic biocontrol agent *Pseudomonas fluorescens* CHA0. *J. Bacteriol.* 180 (12), 3187–3196.
- (33) Scott, S. R., Din, M. O., Bittihn, P., Xiong, L., Tsimring, L. S., and Hasty, J. (2017) A stabilized microbial ecosystem of self-limiting bacteria using synthetic quorum-regulated lysis. *Nat. Microbiol.* 2, 17083.
- (34) Wang, H., Vilela, M., Winkler, A., Tarnawski, M., Schlichting, I., Yumerefendi, H., Kuhlman, B., Liu, R., Danuser, G., and Hahn, K. M. (2016) LOVTRAP: an optogenetic system for photoinduced protein dissociation. *Nat. Methods* 13 (9), 755–758.
- (35) Mukherjee, A., Repina, N. A., Schaffer, D. V., and Kane, R. S. (2017) Optogenetic tools for cell biological applications. *J. Thorac. Dis.* 9 (12), 4867–4870.
- (36) Din, M. O., Danino, T., Prindle, A., Skalak, M., Selimkhanov, J., Allen, K., Julio, E., Atolia, E., Tsimring, L. S., Bhatia, S. N., and Hasty, J. (2016) Synchronized cycles of bacterial lysis for in vivo delivery. *Nature* 536 (7614), 81–85.
- (37) Pu, L., Yang, S., Xia, A., and Jin, F. (2018) Optogenetics manipulation enables prevention of biofilm formation of engineered *Pseudomonas aeruginosa* on surfaces. *ACS Synth. Biol.* 7 (1), 200–208.
- (38) Huang, Y., Xia, A., Yang, G., and Jin, F. (2018) Bioprinting living biofilms through optogenetic manipulation. *ACS Synth. Biol.* 7 (5), 1195–1200.
- (39) Wend, S., Wagner, H. J., Müller, K., Zurbriggen, M. D., Weber, W., and Radziwill, G. (2014) Optogenetic control of protein kinase activity in mammalian cells. *ACS Synth. Biol.* 3 (5), 280–285.
- (40) Nikolados, E. M., Weiße, A. Y., Ceroni, F., and Oyarzún, D. A. (2019) Growth defects and loss-of-function in synthetic gene circuits. *ACS Synth. Biol.* 8 (6), 1231–1240.
- (41) Stirman, J. N., Crane, M. M., Husson, S. J., Gottschalk, A., and Lu, H. (2012) A multispectral optical illumination system with precise spatiotemporal control for the manipulation of optogenetic reagents. *Nat. Protoc.* 7 (2), 207–220.
- (42) Patti, J. M., Allen, B. L., McGavin, M. J., and Höök, M. (1994) MSCRAMM-mediated adherence of microorganisms to host tissues. *Annu. Rev. Microbiol.* 48, 585–617.
- (43) Hmelo, L. R., Borlee, B. R., Almlblad, H., Love, M. E., Randall, T. E., Tseng, B. S., Lin, C., Irie, Y., Storek, K. M., Yang, J. J., Siehnell, R. J., Howell, P. L., Singh, P. K., Tolker-Nielsen, T., Parsek, M. R., Schweizer, H. P., and Harrison, J. J. (2015) Precision-engineering the *Pseudomonas aeruginosa* genome with two-step allelic exchange. *Nat. Protoc.* 10 (11), 1820–1841.
- (44) Horton, R. M., Hunt, H. D., Ho, S. N., Pullen, J. K., and Pease, L. R. (1989) Engineering hybrid genes without the use of restriction enzymes: gene splicing by overlap extension. *Gene* 77 (1), 61–68.
- (45) Gibson, D. G., Young, L., Chuang, R. Y., Venter, J. C., Hutchison, C. A., 3rd, and Smith, H. O. (2009) Enzymatic assembly of DNA molecules up to several hundred kilobases. *Nat. Methods* 6 (5), 343–345.
- (46) Kirienko, N. V., Cezairliyan, B. O., Ausubel, F. M., and Powell, J. R. (2014) *Pseudomonas aeruginosa* PA14 pathogenesis in *Caenorhabditis elegans*. *Methods Mol. Biol.* 1149, 653–669.
- (47) Ni, L., Yang, S., Zhang, R., Jin, Z., Chen, H., Conrad, J. C., and Jin, F. (2016) Bacteria differently deploy type-IV pili on surfaces to adapt to nutrient availability. *NPJ. Biofilms Microbiomes* 2, 15029.